THE ASTROPHYSICAL JOURNAL, 467:579–588, 1996 August 20

ON THE SIZE AND FORMATION MECHANISM OF STAR COMPLEXES IN Sm, Im, AND BCD GALAXIES

BRUCE G. ELMEGREEN,[1] DEBRA MELOY ELMEGREEN,[2] JOHN J. SALZER,[3] AND HEATHER MANN[2]
Received 1994 November 21; accepted 1996 March 6

ABSTRACT

The diameters D_c of the largest star-forming complexes in 67 Magellanic spiral and irregular galaxies and 16 blue compact dwarf (BCD) galaxies are found to scale approximately with the square root of the galaxy luminosity for each type, i.e., smaller galaxies have proportionately smaller star-forming regions. This is the same relation as for the largest complexes in bright spiral galaxies found previously, although Sm/Im galaxies have complexes that, on average, are a factor of ~ 2 larger than the extrapolation for spiral galaxies at the same absolute magnitude, and the BCD galaxies have complexes that are ~ 2 times larger than those typical of the Sm/Im galaxies at the same absolute magnitude. These results are consistent with the interpretation that the largest complexes form at the gravitational length scale in a marginally stable interstellar medium with a nearly constant velocity dispersion $c \sim 5$–10 km s^{-1}. The luminosity scaling is then the result of higher average total densities in smaller galaxies compared with the outer regions of giant spirals. This total density correlation is shown using published H I line widths and optical galaxy sizes.

The implication of these results is that star formation begins when the ratio of the gas density ρ to the total density (gas + stars + dark matter) exceeds several tenths. If star formation lasts for a time scaling with $(G\rho)^{-1/2} \sim D_c/c$, then the main morphological differences between star formation in galaxies of various sizes can be explained: large galaxies have large star complexes that form groups of OB associations slowly for up to 50 Myr; small galaxies have small complexes (in terms of absolute size) that form dense associations quickly, in bursts spanning less than 5 Myr.

Subject headings: galaxies: compact — galaxies: irregular — galaxies: star clusters

1. INTRODUCTION

The process of star formation on large scales may be revealed by correlations between the sizes of the largest star-forming regions and other galaxy properties. Elmegreen et al. (1994, hereafter Paper I) showed that, for 184 spiral galaxies, the diameters D_c of the largest complexes are always comparable to half the fastest growing wavelength of the gravitational instability in a critically stable gas disk, which gives $D_c \sim \pi c R_{25}/2^{1/2}V$ for constant velocity dispersion $c \sim 5$ km s^{-1}, galaxy radius R_{25} at 25 mag arcsec^{-2}, and rotation speed V. We concluded from this that star complexes in the outer parts of spiral galaxies form by gravitational instabilities at the threshold $Q = c\kappa/(\pi G\sigma) \sim 1$ (Kennicutt 1989) for epicyclic frequency κ and disk gas column density σ.

The purpose of the present paper is to determine if this relationship between star formation scale and galactic dynamics also holds for Sm, Im, and BCD galaxies, which have very different rotation and dark matter properties. We measure the sizes of the largest star complexes in 67 small galaxies classified as Magellanic spirals or irregular galaxies (Sm, Im) in the Third Reference Catalogue of Galaxies (de Vaucouleurs et al. 1991), and we do the same for 16 BCD galaxies that were observed as part of a separate study (Salzer et al. 1996a). Good correlations between D_c and absolute galaxy magnitude M_B are found for each galaxy type. We then study the ratios of the optical sizes, $D_{25} = 2R_{25}$, to the H I line widths, W, using Tully (1988) for measurements of H I in Sm/Im galaxies and Salzer et al. (1996b) for H I in BCD galaxies. Another correlation with M_B is found for D_{25}/W. This second correlation implies that Tully-Fisher (1977)–type relationships between total line width, size, and absolute magnitude exist for Sm/Im galaxies, although with larger intrinsic scatter than exhibited by spiral galaxies. The two correlations together suggest that D_c is proportional to D_{25}/W for Sm/Im galaxies, which is similar to the relation for spiral galaxies.

These results give a consistent picture of star formation in which the largest coherent scale is about half the gravitational length at the threshold for interstellar instabilities. The nature of this threshold for Sm/Im galaxies is not obvious. It cannot be the same $Q \sim 1$ threshold as for spirals because Sm/Im galaxies have thick irregular shapes, little rotation, and high dark matter fractions. We suggest instead a more universal criterion for star formation, useful for both Sm/Im galaxies and spirals, that is based primarily on the ratio of the average gas density to the total density in all forms, including gas, stars, and dark matter (Tayler 1976). We show that this criterion follows from $Q \sim 1$ for a spiral galaxy and that it also follows from other instability conditions.

Star complexes are used for this study, rather than H II regions (e.g., Hunter & Gallagher 1986), because star complexes map whole star-forming regions, including stars slightly older than OB stars, whereas H II regions only map the youngest stars. Star complexes are coherent star-forming regions outlined by Cepheid variables, red supergiants, OB associations, and young clusters (Efremov 1978). Almost 90% of all OB associations in nearby galaxies are concentrated into star complexes (Efremov 1995). Star complexes are easily recognized in other galaxies (van den Bergh 1964; Efremov, Ivanov, & Nikolov 1987; Ivanov 1992). Larger galaxies have larger complexes (Paper I), and in

[1] IBM T. J. Watson Research Center, P.O. Box 218, Yorktown Heights, NY 10598.
[2] Vassar College Observatory, Poughkeepsie, NY 12601.
[3] Astronomy Department, Wesleyan University, Middletown, CT 06459.

galaxies the size of ours, where a complex can extend for 1 kpc (such as Gould's Belt), the duration of star formation in a complex can be as long as 5×10^7 yr (Efremov 1989). This is why evolved massive stars are present in star complexes in large galaxies.

The mechanism of star formation on the scale of individual stars is not relevant to the present study. Presumably, stars form in the densest regions of turbulent, self-gravitating clouds after internal energy sources such as random motions and magnetism decay (e.g., Shu, Adams, & Lisano 1987). Here we are more concerned with the formation and evolution of the clouds in which stars eventually appear.

2. STAR COMPLEXES

2.1. *Galaxy Sample and Selection Effects*

The largest star complexes were measured in three samples of galaxies: (1) all Magellanic spiral and irregular galaxies (Sm, Im) listed in the Third Reference Catalogue of Bright Galaxies (RC3) (de Vaucouleurs et al. 1991) with radii $R_{25} > 2'$, (2) all galaxies that appear in the available high-resolution atlases, and (3) a selection of BCD galaxies at low redshift from another study (Salzer et al. 1996a). The Sm/Im galaxies have absolute blue magnitudes down to $M_B = -11$.

The Magellanic spirals and irregulars constitute angular size-limited samples, selected so that even the most distant galaxies in the sample have large complexes that are clearly resolved. Paper I showed that the largest complexes in spirals tend to have diameters of about 5% of the galaxy's diameter, which corresponds to 12″ for a galaxy with a radius of 2′. Such complexes are resolved even on the Palomar Observatory Sky Survey (POSS). In the Sandage & Bedke (1988) atlas, 16 additional Sm/Im galaxies were included with diameters between 1′ and 4′. Because Sm/Im galaxies tend to be intrinsically smaller than spirals, they are, in general, closer than the spiral sample. The BCD galaxies are a random sample. They are low redshift, $z < 0.007$, except for UM 408 with $z = 0.011$, so they represent a similar distance range as the Sm/Im galaxies in our sample.

The largest complexes in Sm/Im galaxies were measured to the nearest 0.5 mm directly from the blue photographs in Part 4 of the Sandage & Bedke (1988) atlas (Parts 1–3 were examined in Paper I), the Revised Shapley-Ames Catalog (NGC 6822, IC 1613, Sex A, SMC, Ho I, and Ho II; Sandage & Tammann 1981), and the Hubble Atlas of Galaxies (NGC 4449, IC 10, and IC 2574; Sandage 1961). Complexes were measured with a 7X ocular to within 0.1 mm on the POSS. The POSS was used only for the anonymous galaxies, except A1240+13, and for NGC 3239 and NGC 3432, which were not in the atlases. The complexes in the BCD galaxies were measured with a cursor off a workstation screen on *B*-band CCD images obtained with the Kitt Peak National Observatory (KPNO) 0.9 m telescope (Salzer et al. 1996a).

The Sandage & Bedke images are all exposed to the same depth, which has a limiting sky magnitude of $B = 23.4$. The reproductions emphasize the outer parts of the galaxies with a limiting apparent radius in the vicinity of 23 mag arcsec^{-2} (Sandage & Bedke 1988). This limit implies that the underlying disks at the positions of the complexes are not clearly visible in the far outer regions (at R_{25}) and so raises the question of whether faint extensions to some complexes could have been missed. We checked for this possible error by plotting scans of intensity through several complexes on CCD images taken with the KPNO 0.9 m telescope as part of a separate study. We also varied the contrast of the images on a video monitor using standard IRAF routines. All of the complexes studied in this way have sharp edges with underlying disks clearly visible. An example of an intensity profile through the *B*-band image of the largest complex in NGC 2366 is shown in Figure 1. We also measured complex sizes off CCD images using cursor positions in IRAF and found that the complex sizes measured from the CCD images were within 10% of the complex sizes measured off the atlas photographs. Thus, for our self-consistent definition of star complexes, we are probably not underestimating the complex sizes by more than a factor of ~ 1.2 using atlas photographs.

To estimate our measuring uncertainties in another way, we compared complex sizes for all of the galaxies in the atlases with POSS measurements of the same complexes. Galaxies in more than one atlas were also compared with each other. In all cases, the measurements of complex diameters were the same on all images to within an rms deviation of 20%.

2.2. *Star Complex Diameters*

There are 46 Magellanic spiral and irregular galaxies in this study and 21 more of this type from Paper I. The diameter, D_c (in parsecs), of the largest complex in each galaxy is listed in Table 1 along with the absolute blue magnitude of the galaxy, M_B, from Tully (1988). The diameter was determined from the square root of the product of the major and minor axes, converted to a linear size by assuming the distance given by Tully (1988). Seven galaxies, indicated by a footnote in the table, did not have M_B listed in Tully, so their absolute magnitudes were determined from the corrected apparent magnitudes B_T^0, using distances from the velocities v_{GSR} (corrected to a general standard of rest) in the RC3, assuming a Hubble constant of 75 km s^{-1} Mpc^{-1}.

Table 2 lists the 16 BCD galaxies examined here, along with their coordinates, absolute magnitudes, and the linear diameters of the largest complexes. The absolute magnitudes were determined from apparent magnitudes obtained through CCD photometry of the images, assuming a Hubble constant of 75 km s^{-1} Mpc^{-1} and using an observed velocity that was corrected to the velocity centroid of the Local Group (Salzer et al. 1996a).

The linear diameters of the complexes are plotted versus the galaxy absolute blue magnitudes in Figure 2. The large dots represent the Magellanic spiral and irregular galaxies, the small dots represent normal spiral galaxies measured in Paper I (i.e., not including the Sm/Im galaxies), and the squares represent BCD galaxies. The complex diameters for the normal spiral galaxies are corrected for inclination angle i by the factor $(\cos i)^{-1/2}$, but the complexes in Sm/Im and BCD galaxies have no inclination corrections. Inclination corrections for Sm/Im galaxies are uncertain because they have intrinsically noncircular shapes and relatively large thicknesses (e.g., Bender & Nieto 1990; Staveley-Smith, Davies, & Kinman 1992). Inclination corrections for Sm/Im galaxy complexes may not even be needed if the complexes are as thick as the main gas disks, which may be several hundred parsecs in galaxies the size of the LMC (Puche et al. 1992).

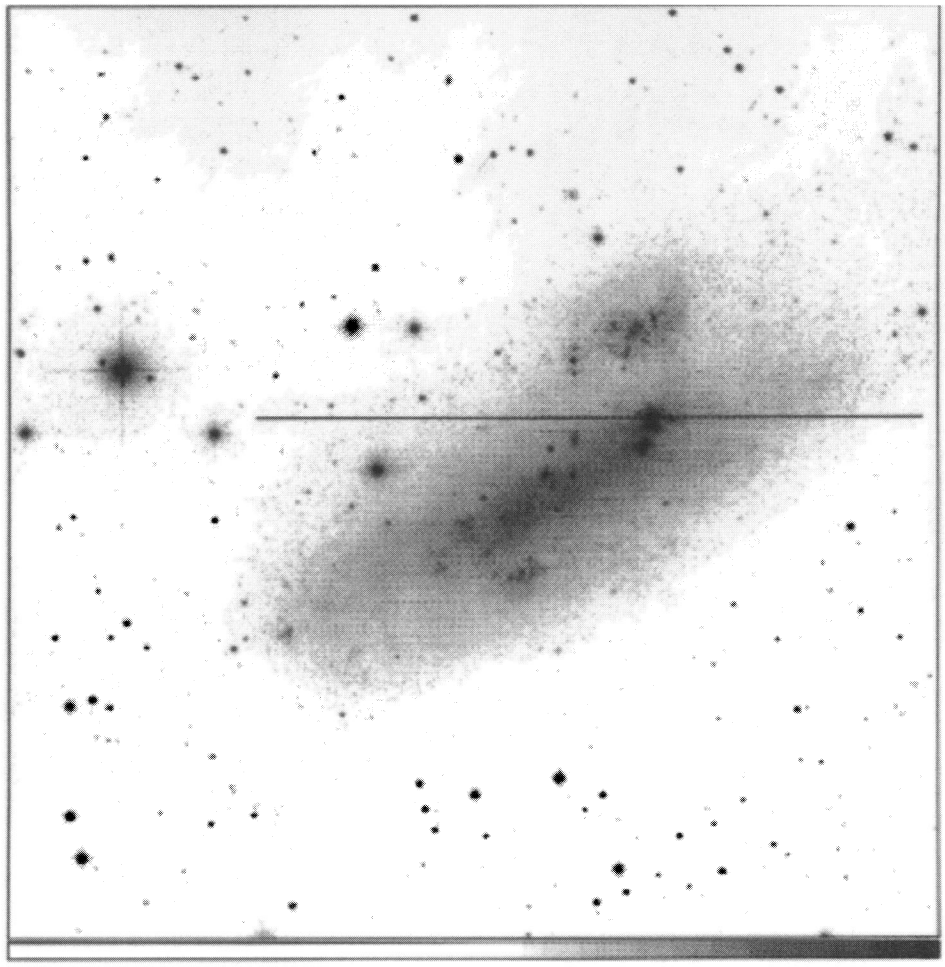

FIG. 1*a*

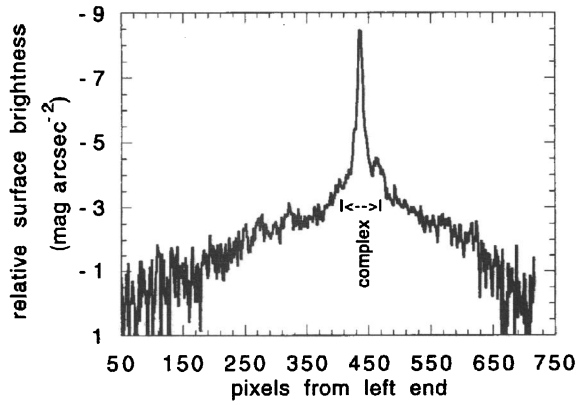

FIG. 1*b*

FIG. 1.—(*a*) *B*-band image of NGC 2366 showing a trace through a complex, with (*b*) intensity profile along the trace. The extent of the complex derived from the square root of the product of the major and minor axes is indicated.

The upper dotted line in Figure 2 represents a least-squares fit to the diameters of all of the galaxies as a function of absolute magnitude, and the lower dashed line represents a least-squares fit to a limiting resolution of 2″ for each galaxy at its assumed distance. With only a few exceptions, the complexes fall well within both limits, so selection and resolution effects do not influence the measurements.

Bivariate least-squares fits to the data are shown separately for the spiral, Sm/Im, and BCD galaxy samples. The mean slopes were determined by first treating M_B as the independent variable and fitting c_1 and a_1 to the equation $\log D_c = c_1 + a_1 M_B$, and then treating $\log D_c$ as the independent variable and fitting c_2 and a_2 to $M_B = c_2 + \log D_c/a_2$; the fitted slope and constant are then $a = (a_1 + a_2)/2$ and $c = (c_1 - c_2 a_2)/2$ for the equation $\log D_c(\mathrm{pc}) = c + aM_B$. This procedure gives

$$\log D_c = -1.47 \pm 1.72 - (0.22 \pm 0.09)M_B \quad \text{(spirals)}, \quad (1)$$

$$\log D_c = -1.16 \pm 0.82 - (0.22 \pm 0.05)M_B \quad \text{(Sm/Im)}, \quad (2)$$

$$\log D_c = -0.31 \pm 0.67 - (0.19 \pm 0.04)M_B \quad \text{(BCD)}, \quad (3)$$

TABLE 1

MAGELLANIC SPIRAL AND IRREGULAR GALAXIES

Galaxy	M_B	D_c (pc)
NGC 55	−18.13	287
NGC 428	−19.14	865
NGC 1156	−17.46	231
NGC 1359	−19.49	731
NGC 1569	−16.37	64
NGC 2188	−17.87	195
NGC 2366	−16.69	825
NGC 2552	−17.47	242
NGC 3109	−16.62	188
NGC 3239	−17.33	916
NGC 3432	−18.38	623
NGC 3510	−16.83	294
NGC 3664	−18.94	746
NGC 4190	−14.04	61
NGC 4214	−17.57	398
NGC 4395	−17.14	337
NGC 4449	−17.66	240
NGC 4597	−19.15	910
NGC 4618	−18.12	346
NGC 4656	−19.21	601
NGC 4861	−18.87	813
NGC 5204	−16.79	188
NGC 5477	−14.76	205
NGC 6822	−15.57	89
A0245+03	−17.28	604
A0246+01	−16.83	457
A0249−01[a]	−17.53	867
A0739+16	−13.21	168
A0956+30	−12.51	46
A0957+05	−14.27	74
A1039+34	−15.94	369
A1155+38	−18.46	1220
A1224+37	−13.15	224
A1225+43	−14.63	98
A1230+31	−14.85	175
A1240+13	−19.10	328
A1246−09	−19.93	2633
A1353+54	−14.82	180
A1417+09	−18.90	1107
A2326+14	−12.63	33
A2327+40	−17.69	425
A2359−15	−14.18	46
IC 10	−16.26	40
IC 1613	−14.30	65
IC 1727	−17.61	364
IC 1953	−19.53	721
IC 2574	−16.37	216
IC 3059[a]	−13.24	81
IC 3239[a]	−14.73	157
IC 3258	−17.53	407
IC 3268	−17.59	438
IC 3355[a]	−11.94	28
IC 3356	−16.23	342
IC 3365	−17.23	203
IC 3412[a]	−15.09	187
IC 3414[a]	−15.67	272
IC 3475[a]	−18.91	306
IC 3583	−17.53	530
IC 3617	−16.99	378
IC 4182	−15.62	352
IC 4662	−16.06	158
IC 5152	−13.69	49
Sex A	−13.85	104
SMC	−16.10	288
Ho I	−15.24	398
Ho II	−17.34	294

[a] Distances for these galaxies were obtained using v_{GSR} from RC3 and a Hubble constant of 75 km s^{-1} Mpc^{-1}.

TABLE 2

BCD GALAXIES

Galaxy	α(1950) (h m s)	δ(1950) (d m s)	M_B	D_c (pc)
I Zw 18	9 30 30	55 27 45	−13.83	192
II Zw 40	5 53 05	03 23 07	−16.17	346
Mk 5	6 53 24	75 40 12	−15.10	304
Mk 36	11 02 15	29 24 36	−13.98	148
Mk 67	13 39 39	30 46 17	−14.37	282
Mk 324	23 24 02	17 59 27	−16.65	665
Mk 328	23 35 09	29 51 10	−16.46	747
Mk 475	14 37 03	37 01 07	−13.64	207
Mk 600	02 48 27	04 14 50	−15.42	392
Mk 750	11 47 28	15 18 05	−14.40	287
Mk 900	21 27 27	02 11 39	−16.86	473
UM 323	01 24 13	−00 54 16	−16.15	496
UM 439	11 34 03	01 05 38	−15.43	193
UM 461	11 48 59	−02 05 40	−14.11	232
UM 462	11 50 03	−02 11 26	−15.73	248
Was 5	10 07 47	22 15 30	−14.05	315

where the statistical errors are $|a_1 - a_2|/2$ and $|c_1 + c_2 a_2|/2$ for the slope and intercept, respectively. Absolute errors for the complex diameters are estimated to be 20% from the measurements and at least 50% from the distance uncertainties. Absolute errors for the magnitudes are probably in the range 0.5–1 mag. However, distance uncertainties affect both D_c and M_B in the same way: for example, if the distance to a galaxy doubles, then M_B changes by −1.5 mag and D_c changes by a factor of 2 for the same galaxy apparent magnitude and complex angular size. Because $\log 2 \approx 0.22 \times 1.5$ mag (cf. eq. [2]), these two changes move the point in Figure 2 nearly parallel to the curve. Thus, distance uncertainties do not significantly affect the scatter in Figure 2. Much of the scatter is probably from intrinsic variabilities in the star formation process.

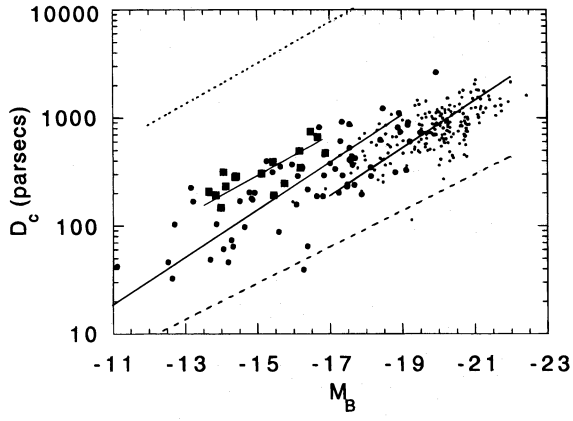

FIG. 2.—The diameters of the largest complexes, D_c, in Sm/Im galaxies (*large dots*) and BCD galaxies (*squares*) are plotted vs. the absolute blue magnitude M_B. The normal spirals studied in Paper I are plotted with small dots. The lines indicate bivariate least-squares fits to the data. The top dotted line indicates the average galaxy diameter D_{25} as a function of absolute magnitude; the bottom dashed line indicates the average seeing-limited size as a function of absolute magnitude, based on a limiting resolution of 2″. All of the measured complexes are well above this seeing limit; some dots appear near the limit because only the average limit is shown and this average is not appropriate for them.

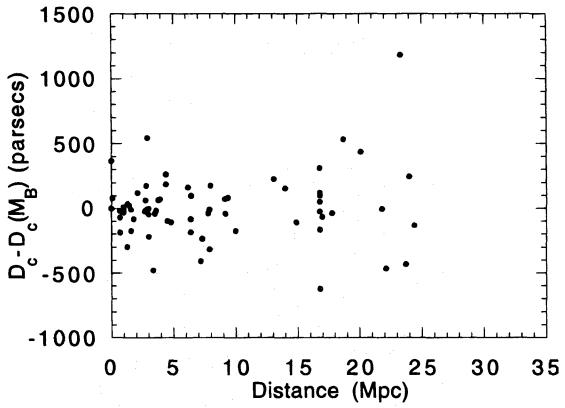

FIG. 3.—The difference between each maximum complex size and the average for a galaxy of that magnitude is shown vs. the distance to the galaxy to demonstrate that there are no systematic biases introduced by resolution limits.

Note that the correlations in Figure 2 are best within each separate galaxy type. The Sm/Im galaxies have ~ 2 times larger complexes than normal spirals for the same extrapolated M_B, and the BCD complexes are a factor of ~ 2 larger than typical Sm/Im galaxies at the same M_B. In terms of galaxy luminosities, L, the slope ~ -0.2 in the above $D_c(M_B)$ relation implies that the complex diameter scales approximately with $L^{0.5}$.

The slope derived in Paper I using the same data as the large galaxy sample was based on a single variable fit, giving $a_1 = -0.14$. The bivariate fit given above is steeper than this single variable fit because the upper and lower cutoffs in D_c are sharper than the upper and lower cutoffs in M_B. Nevertheless, the observations in Paper I were fitted by essentially the same theoretical relations as the current observations.

As a further check against selection effects, Figure 3 shows $D_c - D_c(M_B)$ versus distance for the Sm/Im galaxies, where $D_c(M_B)$ is the fitted function, $-1.16 - 0.22M_B$; the quantity $D_c - D_c(M_B)$ is the deviation from the average. Figure 3 shows that this deviation is independent of distance, which implies that the scatter in Figure 2 is not the result of a distance effect and that there is no obvious bias with distance, as might result from blending, selection, or resolution errors. (The rms deviation in Fig. 3 is smaller for the smaller Sm/Im galaxies, as suggested by Fig. 2, but still independent of distance.)

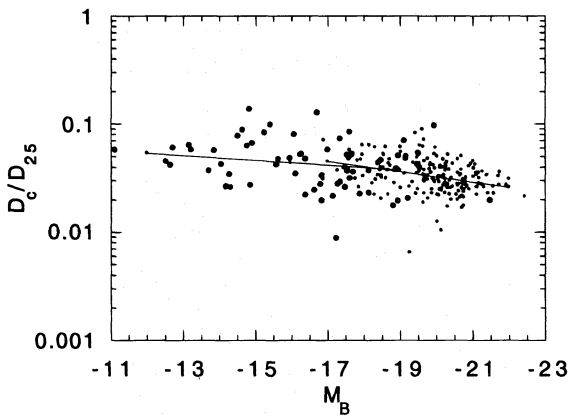

FIG. 4.—The diameters of the largest complexes in the Sm/Im galaxies (*large dots*) are scaled to the galaxy diameters D_{25} and plotted vs. the absolute blue magnitude, with the line indicating a least-squares fit. The normal spirals studied in Paper I have small dots.

Hodge (1983) found a correlation between the characteristic sizes of H II regions in dwarf galaxies (measured as the exponential scale for the size distribution function of the H II regions in each galaxy) and the galaxy absolute magnitude. His fit for H II regions, $\log D_0(\mathrm{pc}) = -1.76 - 0.206M_B$, is similar to ours for star complexes, but the H II regions are a factor of 6 smaller than the complexes at $M_B = -16$. Strobel, Hodge, & Kennicutt (1991) added smaller dwarfs and got a different relation, $\log D_0(\mathrm{pc}) = -0.25 - 0.098M_B$; the reason for this difference is not evident from their data.

Figure 4 shows D_c/D_{25} versus M_B, using the same symbols as in Figure 2. Small galaxies have slightly larger relative complex diameters than large galaxies, which is consistent with the common impression that there are *relatively* large star-forming regions in Sm/Im galaxies. However, the relative size variation is not large, only a factor of ~ 4 for galaxies spanning 11 mag, which is a factor of 10^4 in luminosity.

3. DYNAMICAL PROPERTIES OF Sm/Im AND BCD GALAXIES

In the gravitational instability model for star formation, the complex diameters measured in the previous section should equal some fraction of the fastest growing wavelength of a perturbation in the average interstellar medium. Because this characteristic wavelength depends on galactic properties, particularly on c/κ or cD_{25}/V at the threshold of instability, we investigate these properties here.

Figure 5*a* shows the ratio D_{25}/W_D versus M_B for Sm/Im galaxies in the Nearby Galaxies Catalog (Tully 1988). Figure 5*b* shows W_D and Figure 5*c* shows D_{25}. The velocity W_D is the dynamical profile width parameter in Tully (1988); it is the H I line width with a turbulent component first removed so the residual velocity, which is rotation, can be corrected for inclination; then the turbulent component is added back (see also Tully & Fouque 1985). The diameter D_{25} ($= A_{25}$ in Tully 1988) is corrected for inclination and foreground extinction.

Figures 5*d*–5*f* show analogous BCD galaxy data from a recent study by Salzer et al. (1996b), taken with the Arecibo and KPNO 0.9 m telescopes. In this case, the velocity width is W_{20}, the full H I line width at 20% peak uncorrected for inclination; the diameter is D_{25}, also uncorrected. Inclination and turbulence corrections are not known for BCD galaxies, so we present only the raw data here; corrections will be discussed below.

Bivariate fits to the Sm/Im data are

$$\log W_D(\mathrm{km\ s^{-1}}) = 0.20 \pm 0.60 - (0.11 \pm 0.04)M_B\,, \quad (4)$$

$$\log D_{25}(\mathrm{pc}) = 0.62 \pm 0.43 - (0.19 \pm 0.03)M_B\,, \quad (5)$$

$$\log D_{25}/W_D(\mathrm{pc\ km^{-1}\ s}) = -1.00 \pm 1.16 - (0.16 \pm 0.07)M_B\,. \quad (6)$$

These relations are similar to the Tully-Fisher (1977) relations for larger galaxies that, for our sample, are $W_D = -0.05 \pm 0.44 - (0.13 \pm 0.02)M_B$, $D_{25} = 0.78 \pm 0.42 - (0.18 \pm 0.02)M_B$, and $D_{25}/W_D = -1.02 \pm 1.87 - (0.15$

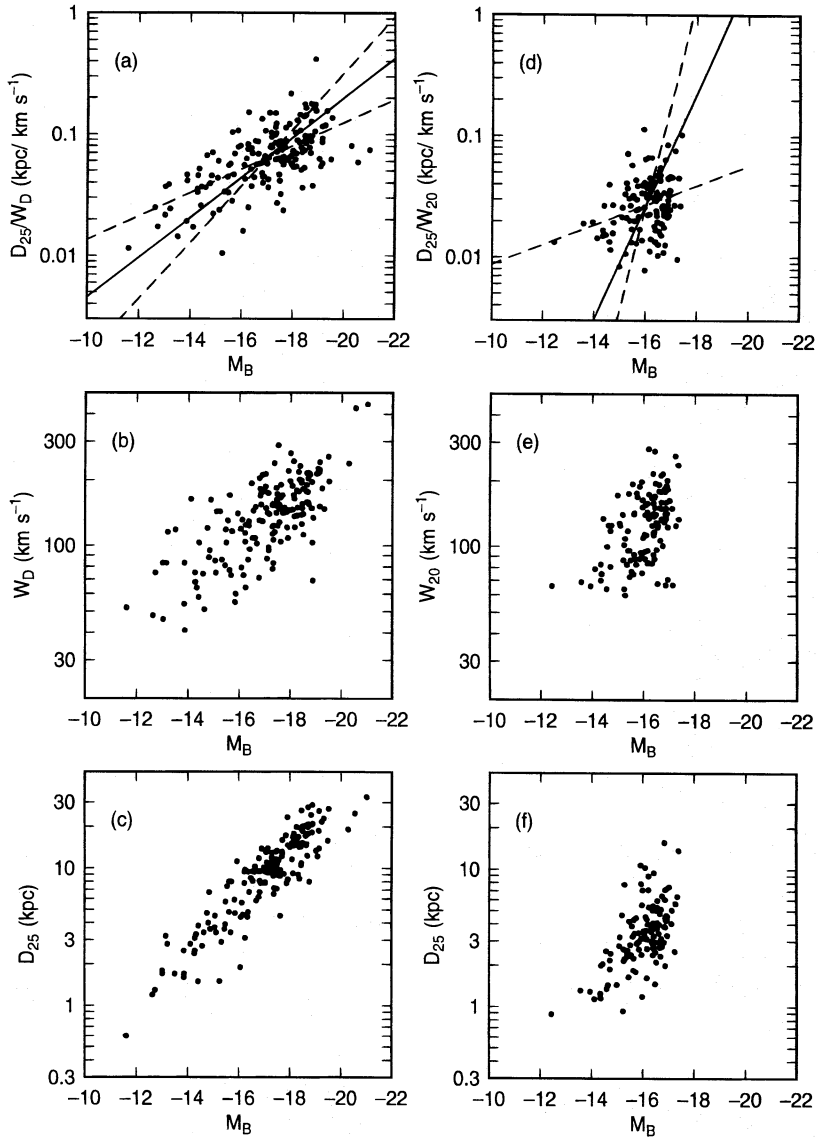

FIG. 5.—(*a*) The galaxy diameter at 25 mag arcsec^{-2} divided by the dynamical profile width parameter is plotted vs. the absolute blue magnitude for all Sm/Im galaxies in Tully (1988); the solid line is the bivariate least-squares fit, and the dashed lines show the extremes from the bivariate fit. (*b*) The velocity width and (*c*) the diameter are also shown. (*d–f*) Same as (*a*)–(*c*), but for BCD galaxies using data from Salzer et al. (1996b).

$\pm 0.10)M_B$, considering all spiral morphologies in Tully (1988).

Bivariate fits to the BCD data are

$$\log W_{20}(\text{km s}^{-1}) = -1.54 \pm 2.22 - (0.23 \pm 0.14)M_B\,, \quad (7)$$

$$\log D_{25}(\text{pc}) = -1.41 \pm 2.21 - (0.31 \pm 0.14)M_B\,, \quad (8)$$

$$\log D_{25}/W_{20}(\text{pc km}^{-1}\text{ s}) = -6.08 \pm 6.21 - (0.47 \pm 0.39)M_B. \quad (9)$$

The uncertainties in these fits are large because the luminosity range for BCD galaxies is small, and the data are uncorrected for inclination and extinction. The main result we obtain from the fit in Figure 5*d* is that the data are *consistent with* the fit to the Sm/Im galaxies in Figure 5*a*. The large scatter in the data preclude drawing any more substantial conclusions.

A variation in D_{25}/W_D with M_B implies that the total density in galaxies increases for smaller galaxies. The density inside D_{25} is $\sim(V_{\rm vir}/R_{25})^2/G$ for virial speed $V_{\rm vir} \approx W_D/2$. This result follows from the virial relation $V_{\rm vir}^2 \propto GM/R$, which gives $(V_{\rm vir}/R)^2 \propto GM/R^3 \propto G\rho_{\rm total}$. Because D_{25}/W_D decreases as M_B increases, smaller and fainter galaxies have higher virial densities.

This result is consistent with the statements by Kent (1987) and Kormendy (1988) that the core densities of dark matter halos increase for galaxies with lower luminosities. It is inconsistent with the claim by Lake, Schommer, & van Gorkom (1990) that the Kent-Kormendy correlation disappears in a larger sample. It is also inconsistent with the results in Binggeli, Sandage, & Tarenghi (1984), who measure a constant core radius (and decreasing core density with lower luminosity), but Kormendy (1985) suggested that the plates used by Binggeli et al. (1984) had poor resolution in the nearly saturated central regions. Evidently, there is no consensus on the dark matter density in galaxies,

which is very difficult to measure compared with the virial density discussed here. If the core density of dark matter is not related to the average total density inside D_{25}, then these other studies are unimportant for our purposes.

Other studies of H I line profiles and optical sizes in Sm/Im and BCD galaxies obtained values of W and D that also show an increase in D/W for fainter galaxies, although this ratio was not considered specifically (e.g., see data in Chamaraux 1977; Shostak 1978; Gordon & Gottesman 1981; Thuan & Seitzer 1979; Thuan & Martin 1981; Longmore et al. 1982; de Vaucouleurs, de Vaucouleurs, & Buta 1983; Kormendy 1985; Hoffman, Helou, & Salpeter 1988).

The reason D_{25}/W_D is smaller in Figure 5*d* for BCD galaxies than in Figure 5*a* for Sm/Im galaxies at a given magnitude is partly because W_{20} is slightly larger for BCD galaxies, but mostly because D_{25} is smaller for BCD galaxies than for Sm/Im galaxies at the same M_B. Such small values of $D_{25}(M_B)$ for BCD galaxies compared with Sm/Im galaxies were previously noted by Hoffman et al. (1989).

4. DISCUSSION

4.1. *Complex Diameters and Galactic Dynamics*

In Paper I, the similarity between the relations D_c versus M_B and R_{25}/V versus M_B for spiral galaxies with rotation speed V was used to infer that $D_c \sim \pi c Q R_{25}/2^{1/2}V$ for turbulent speed $c \sim 5$ km s^{-1} (adjusted to a Hubble constant of 75 km s^{-1} Mpc^{-1}). We get a similar result for the Sm/Im galaxies shown in Figures 2 and 5 if equation (6) is subtracted from equation (2); then $\log D_c = \log D_{25}/W_D - 0.16 - 0.06M_B$, or

$$D_c \sim 6 \text{ km s}^{-1} \frac{D_{25}}{W_D} \quad \text{(Sm/Im)} \tag{10}$$

at $M_B \sim -16$ mag, nearly independent of M_B. The situation is less clear for BCD galaxies because of the relatively large statistical uncertainties in the data. Subtracting equation (9) from equation (3), we get $\log D_c \approx \log D_{25}/W_{20} + 5.77 + 0.28M_B$, or

$$D_c \sim 20 \text{ km s}^{-1} \frac{D_{25}}{W_D} \quad \text{(BCD)} \tag{11}$$

at $M_B \sim -16$ mag, but the statistical uncertainties in the constant are too large to make the result useful.

We would like to understand this result in the context of star formation theory. Next we review the possible origin of star complexes and discuss the nature of the interstellar threshold that may determine when they form.

4.2. *Star Complex Formation and a Density Threshold*

Star complexes are the largest concentrated regions of star formation. They form in the largest gas clouds, which typically have masses of $\sim 10^7\ M_\odot$ (Eggen 1975; Elmegreen 1979). A large fraction of the interstellar gas in a typical spiral galaxy is in these giant clouds (McGee & Milton 1964; Elmegreen & Elmegreen 1983; Rand 1993; Knapen et al. 1993; Garcia-Burillo, Guélin, & Cernicharo 1993), and in the spiral arms most of the molecular mass is associated with them (Grabelsky et al. 1987; Elmegreen & Elmegreen 1987; Digel, De Geus, & Thaddeus 1994). The molecular clouds form OB associations, and as the OB associations age, they disperse and mix with other OB associations from the same large cloud, forming a star complex. When spiral waves are present, these complexes tend to be in the arms, as is most of the other gas and stars; when spiral waves are not present, the complexes are scattered throughout the disk.

Star complexes represent one level in a hierarchy of structures that extends down to stellar aggregates, OB associations, OB subgroups, multiple stellar systems, and, possibly, single stars (Blaauw 1964; Scalo 1985; Efremov 1989, 1995; Efremov & Chernin 1994; Feitzinger & Galinski 1987; Battinelli, Efremov, & Magnier 1996). The hierarchy may also extend to larger scales in the form of clusters of complexes (Feitzinger & Braunsfurth 1984) and star formation spirals (Elmegreen & Efremov 1996). This hierarchical structure suggests that the gas is organized by turbulence and self-gravity, in which case the velocity dispersion and density might vary with the size of the region (e.g., Larson 1981; Scalo 1987, 1990; Falgarone, Puget, & Perault 1992). For spiral galaxies, our selection of star complexes as the largest clearly defined objects containing young stars implies that we have chosen regions whose ages are not so large that shear has significantly distorted them. Elmegreen & Efremov (1996) showed that the size of such a region is usually comparable to the disk thickness, which is $\sim 1/2\pi$ times the unstable wavelength, or $c^2/(\pi G\sigma)$. This scale should apply to galactic-scale star formation whether the star formation process is initiated by a discrete event, such as a gravitational instability in the ambient medium, or by a continuity of events, as in compressible turbulence. Shear is not as important in Sm/Im galaxies as it is in giant spirals, but the characteristic length of the largest scale is still likely to be comparable to the thickness of the gas layer for either a discrete instability or a continuous hierarchy of turbulent structures.

According to this theory, $D_c \sim cR_{25}/V$ in *spiral* galaxies because, at the threshold of collapse, where $Q = c\kappa/(\pi G\sigma) \sim 1$, the gravitational length scale is $c^2/(\pi G\sigma) = cQ/\kappa \sim c/\kappa \sim cQR/(2^{1/2}V)$ for a flat rotation curve. Figures 2 and 5 suggest that complexes in Sm/Im galaxies have a similar property, even though Q is not defined for a thick disk without rotation.

A more general condition that should apply to both spiral and Sm/Im galaxies is that star formation begins when the gas density exceeds a fixed fraction of the total density in the form of gas, stars, and dark matter. This is similar to a suggestion made by Tayler (1976); it follows from considerations of the balance between self-gravity in the gas and galactic tidal and rotational forces. For a disk, the critical density condition is the same as the Q condition, which may be converted into a critical gas density, $\rho_{\rm crit} = \kappa^2/(2\pi G)$, if the critical column density $\sigma_{\rm crit} = \kappa c/(\pi G)$ is converted into a density using the scale height $H = c^2/(\pi G\sigma)$. Because $\kappa = 2^{1/2}V/R$ for a flat rotation curve, the critical gas density is $(V/R)^2/(\pi G)$. For gravitational collapse in an inner Lindblad resonance ring, the critical density is similar, $0.6\kappa^2/G \sim 1.2(V/R)^2/G$ for a rising rotation curve (Elmegreen 1994).

Another example of a density threshold is in a derivation by Spitzer (1942), who wrote the virial relation for a gas cloud in a uniform stellar background as $3V_{{\rm vir},g}^2 = GM_s(R_g)/R_g + \beta GM_g/R_g$, where $V_{{\rm vir},g}$ is the one-dimensional virial velocity of the gas, $M_s(R_g) = 4\pi\rho_s R_g^3/3$ is the stellar mass inside the radius of the cloud R_g, M_g is the gas mass, and β is a constant of order unity that depends on the mass distribution. This equation can be solved for M_g as

a function of R_g, and the maximum stable value of M_g and the maximum stable gas density $\rho_g = 3M_g/(4\pi R_g^3)$ can be determined. The result is the threshold $\rho_g > 2\rho_s/\beta$ for gravitational collapse. Above this threshold, internal turbulent pressure cannot support the cloud against self-gravity and stellar gravity. In terms of the total density, the threshold is $\rho_g > \rho_{\rm total}/(1 + \beta/2)$. In terms of the gas virial velocity and the cloud size, the threshold is $\rho_g > 3(V_{{\rm vir},g}/R_g)^2/(2\pi\beta G)$. The Spitzer (1942) analysis may be closely related to the situation in Sm/Im or BCD galaxies if the stellar density is considered to be stars + dark matter.

Before utilizing these results, we have to convert the observed velocity widths into virial velocities inside the optical diameters. One uncertainty in the interpretation of Figure 5 is that H I diameters are often larger than D_{25} (Huchtmeier, Seiradakis, & Materne 1980, 1981). We use D_{25} because the star formation properties discussed here depend primarily on the total density inside this diameter, where all of the measured star complexes occur. By using W_D or W_{20} from unresolved H I observations and D_{25} from optical observations, we are assuming that the total H I velocity inside D_{25} is not much smaller than the observed H I line width that includes all of the faint emission out to the galaxy edge. Even if the H I extends far beyond the optical disk, this latter assumption will be approximately true if the rotation curve begins to flatten off around or before D_{25}. Otherwise, D_{25}/W could be too low inside D_{25} by perhaps a factor of 2, depending on the additional rise of the rotation curve and total emission outside D_{25}, and on the inclination of the galaxy. To account for this effect, we assume that the one-dimensional virial velocity inside the optical diameter of a Sm/Im galaxy is $W_D/(2\xi)$, and in a BCD galaxy (aside from inclination and extinction effects discussed below), it is $W_{20}/(3.588\xi)$. Here $\xi \sim 1$–2 is the ratio of the line width in the whole, unresolved galaxy to the line width inside the optical diameter. The factor of $\frac{1}{2}$ in the first expression is from Tully's (1988) definition of W_D as a full dynamical width. The factor of 1/3.588 in the second expression converts a full width at 20% peak to a dispersion for a Gaussian profile.

We should also correct the BCD line widths and diameters for inclination and extinction. Let us suppose the H I line widths consist of turbulent and rotational components, v_t (in one dimension) and v_r, respectively. The observed Gaussian velocity dispersion is then $V_{\rm obs} \approx (v_t^2 + v_r^2 \sin^2 i)^{1/2}$ for inclination i. The one-dimensional virial velocity is $V_{\rm vir} \approx (v_t^2 + v_r^2/3)^{1/2}$. The factor of 3 in the second expression is from the assumption that the one-dimensional virial speed squared is $\frac{2}{3}$ the total kinetic energy per unit mass. Writing $X = (v_r/v_t)^2$, the ratio of these quantities is $V_{\rm vir}/V_{\rm obs} = [(1 + X/3)/(1 + X \sin^2 i)]^{1/2}$. The average value of $\sin^2 = 0.5$, so the ratio of the rms velocities is $\langle V_{\rm vir}^2\rangle^{1/2}/\langle V_{\rm obs}^2\rangle^{1/2} \approx [(1 + X/3)/(1 + X/2)]^{1/2}$. This ratio varies by only a small amount, between 0.9 and 0.8, for X in the range of 1–100 from Sm/Im to giant galaxies. Thus, at each M_B, the average of the uncorrected velocity dispersions that come from W_{20} in Figure 5*e* should be 10%–20% larger than the one-dimensional virial velocity. This inclination correction to W_{20} is likely to be compensated by a similar increase in D_{25} when extinction is removed. Thus, D_{25}/W_{20} without corrections should be approximately equal to $D_{25}/(3.588\xi V_{\rm vir})$ with extinction and inclination corrections.

Now we take Spitzer's (1942) result for the whole interstellar medium in a Sm/Im galaxy by setting $R_g \sim R_{25}$; then at the threshold for collapse, $\rho \sim 3(V_{\rm vir}/R_{25})^2/(2\pi\beta G)$. We also assume, as in Paper I, that the largest complexes have diameters equal to $\frac{1}{2}$ the Jeans length, $D_c = 0.5c/(G\rho/\pi)^{1/2}$. Then for Sm/Im galaxies,

$$D_c \sim \pi(\beta/6)^{1/2} cR_{25}/V_{\rm vir} \sim \pi\xi(\beta/6)^{1/2} cD_{25}/W_D \quad (12)$$

for β of order unity. Equations (10) and (12) suggest that $\pi\xi(\beta/6)^{1/2}c \sim 6$ km s^{-1} or $c \sim 5/(\xi\beta^{1/2})$ km s^{-1} for Sm/Im galaxies with a wide range of M_B.

For BCD galaxies, the primary difference is in the conversion from $V_{\rm vir}$ to W_{20},

$$D_c \sim \pi(\beta/6)^{1/2} cR_{25}/V_{\rm vir} \sim 1.8\pi\xi(\beta/6)^{1/2} cD_{25}/W_{20} . \quad (13)$$

Equations (11) and (13) suggest that $1.8\pi\xi(\beta/6)^{1/2}c \sim 20$ km s^{-1} for $M_B \sim -16$ mag, which gives $c \sim 9/(\xi\beta^{1/2})$ km s^{-1} for BCD galaxies. Note that ξ and β could be different for BCD and Sm/Im galaxies, and that this result has a huge statistical uncertainty for BCD galaxies.

We return now to the correlation in Figure 4. The above results suggest that, in gas-rich galaxies, the complex diameter scales with the local Jeans length for an interstellar medium that is marginally stable. Then the implied relation $D_c \propto cD_{25}/V_{\rm vir}$ may be inverted to give the relative complex size, $D_c/D_{25} \sim c/V_{\rm vir}$, multiplied by some constant close to unity. For a thin disk with a flat rotation curve $V(R)$ and $Q = 1$, the exact relation would be $D_c/D_{25} = (\pi/8^{1/2})c/V(R_{25})$. If follows that D_c/D_{25} scales almost exclusively with $1/V$ if c is constant. Actually, the difference between a flat rotation curve and a solid-body rotation curve introduces an additional factor of $2^{1/2}$, so D_c/D_{25} varies from some constant times c/V for large galaxies with flat rotation curves to about the same constant times $c/(2^{1/2}V)$ for small Sm/Im galaxies, which tend to have solid-body rotation curves throughout a large fraction of their visible disks. Now the gradual slope in Figure 4 may be explained. The rotational velocities in the most luminous spiral galaxies are about 250 km s^{-1}, and the total (rotational + random) velocities in the smallest galaxies are about 40 km s^{-1} (Puche et al. 1992; Martinbean & Carignan 1994; Skillman 1994). Thus, the virial velocities change with absolute magnitude by about a factor of 6 over the whole range in Figure 4, so the relative complex size should change with luminosity by about a factor of $6/2^{1/2} = 4$, as observed.

5. CONCLUSIONS AND IMPLICATIONS

The size of the largest star complex in a galaxy scales with the ~ 0.5 power of the galaxy luminosity for spirals, Magellanic spiral, and irregular galaxies, and possibly BCD galaxies; each type has a slightly different constant of proportionality. The relative size of the largest star complex in a galaxy, compared with the galaxy size, is about constant from galaxy to galaxy, decreasing by a factor of only ~ 4 from small Sm/Im galaxies to large spiral galaxies. These scaling laws are consistent with the largest complex size equal to $\frac{1}{2}$ of the characteristic Jeans length in the ambient gas if the gas velocity dispersion is always the same in normal galaxies, around 5–10 km s^{-1}, and the gas density is always near the threshold for instability. The scaling of the Jeans length with the galaxy luminosity results from a systematic variation of the mean virial density of a galaxy with its luminosity, as implied by the Tully-Fisher relations.

The intrinsic and statistical variations in the measurements of D_c for complexes and D/W for galaxies are too large at the present time to use complex diameters as a direct probe of gas velocity dispersions or critical densities. The theoretical constants of proportionality that relate these quantities to the gravitational length scale are also uncertain, and likely to vary between galaxies as the mass distribution and other properties vary. Nevertheless, the star complex data are consistent with the hypothesis that star formation on the largest scale tends to occur at the gravitational length for reasonable gas parameters. The data also suggest that similar star formation processes operate in galaxies over a wide range of luminosities, with scale differences resulting primarily from systematic changes in the underlying galactic mass distributions.

If this hypothesis is correct, then we are led to the following picture of star formation: Most star formation is initiated by turbulence compression and gravitational instabilities in a marginally stable interstellar medium. The largest obvious length scale is comparable to the disk thickness, which is about the Jeans length in the ambient medium. Stars form in the dense cores of clouds having this scale, and they appear in the form of clusters and OB associations that are concentrated into star complexes.

The timescale for star formation in each complex also follows from this picture, being approximately equal to the Jeans time, or the Jeans length divided by the velocity dispersion. This result comes from the timescale for turbulent energy dissipation ($\sim L/c$) as well as from the self-gravitational timescale $(G\rho_{\rm gas})^{-1/2}$. Direct evidence for this timescale dependence on size is in Elmegreen & Efremov (1996). For a threshold gas density proportional to the total density in all forms (§ 4.2), the timescale for star formation on the gravitational length scale decreases for smaller galaxies.

There are important observational implications for such a systematic decrease in star formation timescale with galaxy size. In galaxies like the Milky Way, the timescale for star formation is long, 5×10^7 yr (Efremov 1995), primarily because the gravitational length is large, ~ 1 kpc. This means that star formation persists in a region for a time longer than the lifetime of an O-type star, so star-forming regions contain both evolved stars (red supergiants and Cepheid variables) and OB stars from the current activity. In small galaxies, the ratio of the gravitational length to the turbulent speed is small, possibly only 5×10^6 yr, so essentially all of the complex forms during the lifetime of a single O star (e.g., see Lequeux et al. 1981). This result follows entirely from our observation that star complexes are systematically smaller in smaller galaxies, considering a nearly constant gaseous velocity dispersion.

The implication is that star-forming regions in small galaxies tend to be much brighter, but not much larger relative to the host galaxy, than star-forming regions in giant spirals. This result may explain why the luminosity functions of H II regions are shallower in small galaxies than in large galaxies (Smith & Kennicutt 1989).

D. M. E. and B. G. E. gratefully acknowledge support from NSF grant AST-9201640. D. M. E., J. J. S., and H. M. thank the Keck Foundation and Vassar URSI program for support. We thank B. Tully for an electronic copy of the Nearby Galaxies Catalog.

REFERENCES

Battinelli, P., Efremov, Yu. N., & Magnier, E. A. 1996, A&A, in press
Bender, R., & Nieto, J. L. 1990, A&A, 239, 97
Binggeli, B., Sandage, A., & Tarenghi, M. 1984, AJ, 89, 64
Blaauw, A. 1964, ARA&A, 2, 213
Chamaraux, P. 1977, A&A, 60, 67
de Vaucouleurs, G., de Vaucouleurs, A., & Buta, R. 1983, AJ, 88, 764
de Vaucouleurs, G., de Vaucouleurs, A., Corwin, H. G., Jr., Buta, R., Paturel, G., & Fouque, P. 1991, Third Reference Catalogue of Bright Galaxies (New York: Springer)
Digel, S., De Geus, E., & Thaddeus, P. 1994, ApJ, 422, 92
Efremov, Yu. N. 1978, Soviet Astron. Lett., 5, 12
———. 1989, Space Phys. Rev., 7, 105
———. 1995, AJ, 110, 2757
Efremov Yu. N., & Chernin A. D. 1994, Vistas Astron., 38, 165
Efremov, Yu. N., Ivanov, G. R., & Nikolov, N. S. 1987, Ap&SS, 135, 119
Eggen, O. J. 1975, PASP, 87, 37
Elmegreen, B. G. 1979, ApJ, 231, 372
———. 1994, ApJ, 425, L73
Elmegreen, B. G., & Efremov, Yu. N. 1996, ApJ, 466, 802
Elmegreen, B. G., & Elmegreen, D. M. 1983, MNRAS, 203, 31
———. 1987, ApJ, 320, 182
Elmegreen, D. M., Elmegreen, B. G., Lang, C., & Stephens, C. 1994, ApJ, 425, 57 (Paper I)
Falgarone, E., Puget, J. L., & Perault, M. 1992, A&A, 257, 715
Feitzinger, J. V., & Braunsfurth, E. 1984, A&A, 139, 104
Feitzinger, J. V., & Galinski, T. 1987, A&A, 179, 249
Garcia-Burillo, S., Guélin, M., & Cernicharo, J. 1993, A&A, 274, 123
Gordon, D., & Gottesman, S. T. 1981, AJ, 86, 161
Grabelsky, D. A., Cohen, R. S., May, J., Bronfman, L., & Thaddeus, P. 1987, ApJ, 315, 122
Hodge, P. W. 1983, AJ, 88, 1323
Hoffman, G. L., Helou, G., & Salpeter, E. E. 1988, ApJ, 324, 75
Hoffman, G. L., Helou, G., Salpeter, E. E., & Lewis, B. M. 1989, ApJ, 339, 812
Huchtmeier, W. K., Seiradakis, J. H., & Materne, J. 1980, A&A, 91, 341
———. 1981, A&A, 102, 134
Hunter, D. A., & Gallagher, J. S. 1986, PASP, 98, 5
Ivanov G. R. 1992, MNRAS, 257, 119
Kennicutt, R. C. 1989, ApJ, 344, 685
Kent, S. M. 1987, AJ, 91, 1301
Knapen, J. H., Cepa, J., Beckman, J. E., Soledad Del Rio, M., & Pedlar, A. 1993, ApJ, 416, 563
Kormendy, J. 1985, ApJ, 295, 73
———. 1988, in Origin, Structure and Evolution of Galaxies, ed. Fang Li Zhi (Singapore: World Scientific), 252
Lake, G., Schommer, R. A., & van Gorkom, J. H. 1990, AJ, 99, 547
Larson, R. B. 1981, MNRAS, 194, 809
Lequeux, J., Maucherat-Joubert, M., Deharveng, J. M., & Kunth, D. 1981, A&A, 103, 305
Longmore, A. J., Hawarden, T. G., Goss, W. M., Mebold, U., & Webster, B. L. 1982, MNRAS, 200, 325
Martinbean, N., & Carignan, C. 1994, AJ, 107, 543
McGee, R. X., & Milton, J. A. 1964, Australian J. Phys., 17, 128
Puche, D., Westpfahl, D., Brinks, E., & Roy, J. R. 1992, AJ, 103, 1841
Rand, R. J. 1993, ApJ, 410, 68
Salzer, J. J., Elston, R., Sudarsky, D., & Sinnott, K. 1996a, in preparation
Salzer, J. J., Rosenberg, J. L., Weisstein, E., Mazzarella, J. M., & Bothun, G. D. 1996b, in preparation
Sandage, A. 1961, The Hubble Atlas of Galaxies (Washington: Carnegie Institution of Washington)
Sandage, A., & Bedke, J. 1988, Atlas of Galaxies (Washington: GPO)
Sandage, A., & Tammann, G. A. 1981, A Revised Shapley-Ames Catalog of Bright Galaxies (Washington: Carnegie Institution of Washington)
Scalo, J. M. 1985, in Protostars and Planets II, ed. D. C. Black & M. S. Matthews (Tucson: Univ. Arizona Press), 201
———. 1987, in Interstellar Processes, ed. D. J. Hollenbach & H. A. Thronson Jr. (Dordrecht: Reidel), 439
———. 1990, in Physical Processes in Fragmentation and Star Formation, ed. R. Capuzzo-Dolcetta, C. Chiosi, & A. Di Fazio (Dordrecht: Kluwer), 151
Shostak, G. S. 1978, A&A, 68, 321
Shu, F. H., Adams, F. C., & Lisano, S. 1987, ARA&A, 25, 23
Skillman, E. D. 1994, in Violent Star Formation from 30 Doradus to QSOs, ed. G. Tenorio-Tagle (Cambridge: Cambridge Univ. Press), 168
Smith, T. R., & Kennicutt, R. C. 1989, PASJ, 101, 649
Spitzer, L., Jr. 1942, ApJ, 95, 329

Stavely-Smith, L., Davies, R. D., & Kinman, T. D. 1992, MNRAS, 258, 334
Strobel, N. V., Hodge, P., & Kennicutt, R. C. 1991, ApJ, PASP, 102, 1241
Tayler, R. J. 1976, MNRAS, 177, 39
Thuan, T. X., & Martin, G. E. 1981, ApJ, 247, 823
Thuan, T. X., & Seitzer, P. O. 1979, ApJ, 231, 327
Tully, R. B. 1988, Nearby Galaxies Catalog (Cambridge: Cambridge Univ. Press)
Tully, R. B., & Fisher, J. R. 1977, A&A, 54, 661
Tully, R. B., & Fouque, P. 1985, ApJS, 58, 67
van den Bergh, S. 1964, ApJS, 9, 65